ACS APPLIED MATERIALS & INTERFACES

RESEARCH ARTICLE

www.acsami.org

Simultaneous Analysis of Optical and Mechanical Properties of Cross-Linked Azobenzene-Containing Liquid-Crystalline Polymer Films

Aki Shimamura,[†] Arri Priimagi,[†] Jun-ichi Mamiya,[†] Tomiki Ikeda,[*,†] Yanlei Yu,[‡] Christopher J. Barrett,[§] and Atsushi Shishido[*,†]

[†]Chemical Resources Laboratory, Tokyo Institute of Technology, R1-12, 4259 Nagatsuta, Midori-ku, Yokohama 226-8503, Japan

[‡]Department of Materials Science, Fudan University, 220 Handan Road, Shanghai 200433, China

[§]Department of Chemistry, McGill University, Montreal, Quebec, Canada H3A 2K6

ABSTRACT: The photomechanical behavior of cross-linked azobenzene-containing liquid-crystalline polymer films was investigated by means of simultaneous measurement of their optical and mechanical properties. The connection between photoisomerization of the azobenzene moieties, photoinduced change in molecular alignment, photoinduced stress generation, and macroscopic bending was analyzed. Upon UV irradiation, the films exhibited bending due to gradient in *cis*-azobenzene content, and subsequent unbending when *cis*-azobenzene content became uniform throughout the film. The maximum photoinduced stress was generated in the same time scale as the time required to reach photostationary state in the *cis*-azobenzene concentration. The maximum values of photogenerated stress strongly depended on the crosslinker concentration, even if the azobenzene concentration and the *cis*-azobenzene content in the photostationary state were similar for all the polymer films. The stress is connected to the initial Young's modulus and also to the photoinduced change in birefringence of the polymer films. In addition, a significant photoinduced decrease in Young's modulus was for the first time observed in cross-linked azobenzene-containing liquid-crystalline polymers, which is likely to be an important factor in dictating their photomechanical behavior.

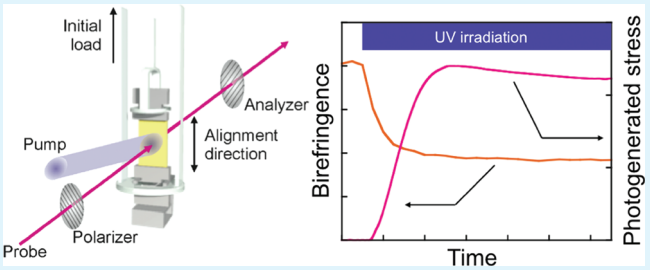

KEYWORDS: azobenzene, photomobile materials, photomechanics, Young's modulus, photosoftening

1. INTRODUCTION

Azobenzene-containing polymers are a fascinating class of photochromic materials due to the multitude of photoinduced effects brought about by the photoisomerization of azobenzene.[1] Indeed, azobenzene is a unique photoswitch, providing a toolkit for studying, e.g., photobiological phenomena as well as for controlling the optical and holographic properties of the material systems into which they are incorporated.[2−4] Perhaps most remarkably, the molecular-level photoisomerization can also give rise to macroscopic deformation of the material system, allowing one to convert light energy directly into mechanical work (photomobile materials) as well as to inscribe photoinduced surface-relief structures.[5,6] These photomechanical effects extend the applicability of azobenzene-containing polymers towards photodriven actuators and artificial muscles, as well as to one-step fabrication techniques of diffractive optical elements.

Since the first demonstrations of photocontraction in liquid-crystal (LC) elastomers in early 2000s,[7−9] the photomobile behavior of azobenzene-based polymer materials has attained significant attention. In particular, precisely controlled and reversible three-dimensional movements such as photoinduced bending are expected to find applications as photomobile actuators, micromechanical components and artificial muscles.[10−14] Being nondestructive and noncontact, and providing high spatial and temporal resolution, light makes an ideal trigger for externally controllable actuators. The most promising class of materials for photoinduced actuation is cross-linked azobenzene-containing LC polymers. In such polymers, the photoisomerization of the azobenzene moieties from the rodlike trans-state to the bent cis-state destructs the initial LC alignment, which in turn generates the sufficiently strong strain required to deform the polymer film.[5] Depending on the material design and experimental configuration, different types of photoinduced motions such as oscillation, swimming, rotation, and inchworm movement can be induced.[15−19]

The photoinduced bending of cross-linked azobenzene-containing LC polymers is conceptually quite simple: the process is driven by gradient in the isomerization-induced reduction in the LC order, which results in asymmetric deformation and bending of the film. However, the process is highly sensitive to, e.g., initial mesogen alignment[20,21] and cross-linker concentration of the polymer network. The cross-linking density changes Young's modulus and the thermomechanical properties of the material system in a delicate manner, playing an important role in the

Received: May 17, 2011
Accepted: October 21, 2011
Published: October 21, 2011

mobility of the polymer segments.[22] However, the cross-linker concentration dependence is different in high-azobenzene-concentration and low-azobenzene-concentration polymers. For the former, i.e., if the penetration depth of the incident light is low, both the photogenerated stress and the bending efficiency have been reported to increase with crosslinker concentration.[23−25] On the other hand, in the case of low azobenzene concentration, a low cross-linker concentration is favorable for optimizing the photoinduced/thermally induced deformation of cross-linked LC polymers.[22,26] We recently showed that the maximum photogenerated mechanical stress is obtained in material systems bearing a moderate concentration of azobenzene cross-links, supplemented with higher density of nonphotoactive crosslinks.[27] However, the relation between the time dynamics of photoisomerization and the photomechanical properties has not been investigated in detail because of the high absorbance of the azobenzene-containing polymer films. Considerable effort has been put into modeling the photomechanical properties of cross-linked azobenzene-containing LC polymers, and in some cases, good agreement has been obtained between analytical models and experimental results.[28−31] However, the effect of structure−property relationships and crosslinking density on the photochemical and photomechanical properties of azobenzene-containing cross-linked LC polymers is not yet well understood, and gaining such understanding would be important for rational design and optimization of the performance of polymer actuators and artificial muscles.

In this study, simultaneous measurements of photoisomerization, photoinduced change in birefringence and photogenerated stress in cross-linked LC polymer films with low azobenzene concentration were performed, in order to quantitatively understand the relationship between their optical and photomechanical properties. It has been found that the production of *cis*-azobenzenes induces a change in birefringence, which is directly connected to the generation of stress within the films. The photogenerated stress depended strongly on the initial Young's modulus of the films, which was affected by the crosslinking density, and also by photoinduced change in birefringence. In addition, significant photoinduced decrease in Young's modulus (photosoftening) of the films was observed for the first time, which might be a new factor contributing to their photomechanical properties.

2. EXPERIMENTAL SECTION

Preparation of Cross-Linked LC Polymer Films. We prepared three cross-linked azobenzene-containing LC polymer samples with different crosslinker concentrations but fixed concentrations of the azobenzene moieties. To evaluate the temporal change in *cis*-azobenzene content by UV−vis spectroscopy, the azobenzene concentration was set to 5 mol % in all samples. The chemical structures of the compounds used are shown in Figure 1, and the abbreviations and the feed ratios of the samples are given in Table 1. The constituent compounds were synthesized according to previously reported methods.[32,33] The samples were prepared by in situ photopolymerization of the mixtures of the compounds, using 2 mol % of a photoinitiator (Ciba Specialty, Irgacure 784). The mixtures were melted at 110 °C and injected into 10 and 20 μm thick glass cells, coated with rubbed polyimide (JSR, AL1254) in order to obtain homogeneous mesogen alignment. The mixtures were cooled to an LC phase temperature using a cooling rate of 0.1 °C/min (**P20**, polymerization temperature 50 °C) or 0.5 °C/min (**P60** and **P100**, polymerization temperature 60 °C). Photoirradiation was carried out using a 500-W high-pressure mercury lamp (Ushio, UI-501HQ) equipped with glass filters (AGC techno glass, Y-52 and IRA-25S). The irradiation intensity was 2.0 mW/cm^2 and the polymerization time was 2 h. The polymerized samples were removed from the glass cells, rinsed in ethyl acetate to remove any unreacted monomers, and dried overnight under reduced pressure.

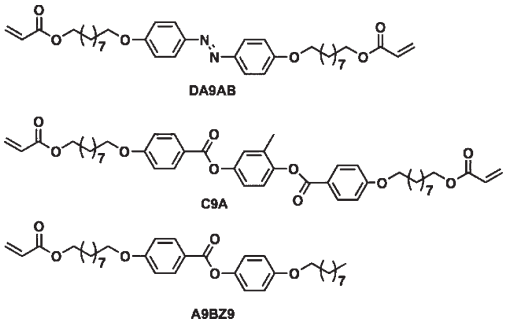

Figure 1. Chemical structures of the compounds used in this study.

Table 1. Nomenclature and Feed Ratio (mol %) of the Compounds

	cross-linker		
sample	**DA9AB**	**C9A**	monomer **A9BZ9**
P20	5	15	80
P60	5	55	40
P100	5	95	0

Characterization Methods. The mesogen alignment at room temperature was evaluated by polarized optical microscopy (Olympus, BH-2), polarized UV−vis spectroscopy (Jasco V-650), and polarized FTIR spectroscopy (Jasco FT/IR-6100). To evaluate the *cis*-azobenzene content of the samples upon UV irradiation, we employed the Fischer's method using two photostationary states generated by excitation wavelengths of 365 and 405 nm.[34] The thermodynamic properties of the samples were evaluated with a differential scanning calorimeter (DSC Seiko Instruments, EXTRAR6000, DSC6220G), using heating and cooling rates of 10 °C/min. At least three scans were performed to check the reproducibility. The phase behavior of the polymers was determined by simultaneous measurement of X-ray diffraction patterns and DSC curves (Rigaku, XRD-DSC).

Photoresponsive Behavior and Mechanical Properties. Photoinduced bending of the films was induced by irradiation with unpolarized light from a 365 nm UV-LED (Keyence, UV-400 with UV-50H and L-8) at room temperature. The bending behavior was monitored with a digital camera (Omron, VC-HRM20Z and VC1000). We used time dynamics of the bending angle (determined by drawing a line between the mounting point and the tip of the film and calculating the angle with respect to the vertical direction) to quantify the bending behavior.

The experimental setup for the evaluation of the photoinduced changes in birefringence and stress is shown in Figure 2. The intensity of a probe beam from a 633 nm He−Ne laser (Melles Griot, 05-LHR-151) was monitored with a photodiode through a polarizer/sample/analyzer configuration, with the transmission directions of the polarizer/analyzer set to ±45° with respect to the alignment direction of the mesogens. The photoinduced change in birefringence (Δn) was estimated from the transmittance (T) using the equation

$$T = \sin^2\left(\frac{\pi d \Delta n}{\lambda}\right) \quad (1)$$

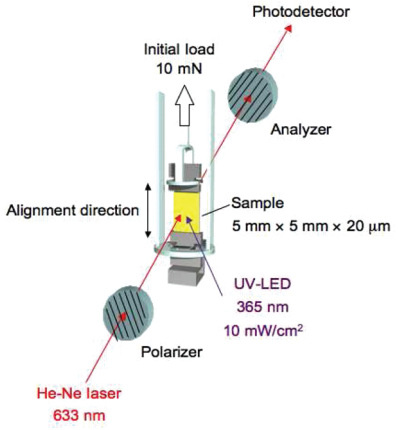

Figure 2. Schematic illustration of the experimental setup for evaluating the photoinduced change in molecular alignment and the photoinduced stress of the samples.

where d is the film thickness and λ is the wavelength of the probe beam. The photoinduced stress was measured with a thermomechanical analyzer (TMA, Shimadzu, TMA-60) by clamping the films at both ends (see Figure 2) and using an initial load of 10 mN in the mesogen alignment direction. Young's moduli of the samples in the mesogen alignment direction were determined from the stress−strain curves of the TMA measurements both before and during UV irradiation (365 nm, 10 mW/cm^2). For the UV-irradiated films, the measurements were performed in the photostationary state in order to eliminate the effect of photoinduced contraction on the stress−strain curves. The tensing rate was 20 mN/min.

3. RESULTS AND DISCUSSION

The cross-linked azobenzene-containing LC polymers studied in this work contain equal azobenzene content (5 mol %) but differ in the concentration of the nonphotoactive crosslinker **C9A** (see Figure 1). This allows us to tune the room-temperature elastic modulus of the samples while keeping absorbance of the films the same: the absorbance of 10 μm thick samples at 365 nm for unpolarized light was around unity. Young's moduli were 70, 100, and 170 MPa for **P20**, **P60**, and **P100**, respectively. The mesogen alignment was evaluated using polarized optical microscopy and polarized UV−vis/IR absorption spectroscopy. To avoid overly high absorbance of the samples at around 360 nm, the spectroscopic studies were performed using samples photopolymerized in a 10 μm cell, whereas a 20 μm cell was used for the photomechanical characterization of the cross-linked azobenzene-containing LC polymers. Figure 3 exemplifies the results for **P20**: the sample exhibits a bright image between crossed polarizers when the director axis is set to ±45° with respect to the analyzer and an opaque image when the axes coincide (Figure 3a), indicating homogeneous mesogen alignment. Figure 3b and c display the polarized UV−vis and IR spectra, respectively. The $\pi\pi^*$ transition of the azobenzene moieties and the stretching vibration of the benzene rings at 1608 cm^{-1} are evidence that both the azobenzene mesogens and the nonphotoresponsive mesogens (**C9A** and **A9BZ9**) are highly aligned along the rubbing direction. The phase behavior, the order parameters determined from UV−vis and IR spectra, as well as the *cis*-azobenzene content upon UV irradiation (365 nm, 10 mW/cm^2) and Young's moduli of the samples are presented in Table 2. The order parameter of **P20** is higher than for **P60** and **P100**, which can be attributed to the fact that

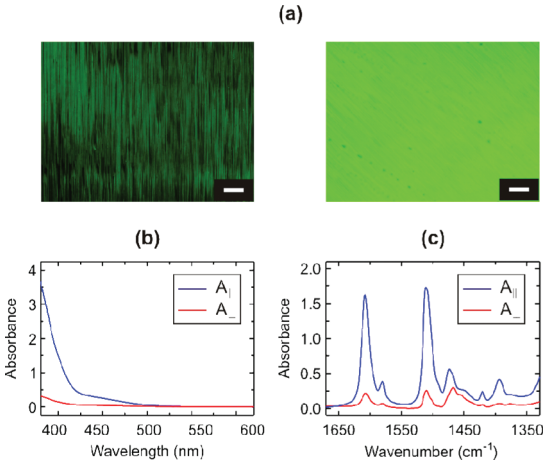

Figure 3. (a) Polarized optical micrographs for **P20**, taken at 0° (left) and 45° (right) angles between the polarizer and the rubbing direction. The scale bar corresponds to 200 μm. (b) Polarized UV−vis and (c) IR spectra for **P20**. $A_{||}$ and $A_{\perp}$ correspond to absorption parallel and perpendicular to the rubbing direction, respectively.

Table 2. LC Phase Behavior, Order Parameters, Initial Birefringence, *cis*-Azobenzene Content in the Photostationary State, and Young's Modulus in the Absence of UV Irradiation for P20, P60, and P100

sample	phase transition temperatures (°C)	order parameter (UV−vis/IR)	initial birefringence	*cis*-azobenzene content (%)	elastic modulus (MPa)
P20	G41 SmA 140 N	0.75/0.69	0.154	59	70
P60	G 38 N > 200	0.63/0.5	0.137	61	100
P100	N>200	0.61/0.49	0.140	54	170

P20 exhibits a Smetic A phase whereas **P60** and **P100** show a nematic phase. **P20** and **P60** exhibited a base line shift due to a glass transition at around room temperature, while **P100** showed neither base line shift nor peaks. Even if the crosslinker content is varied, we observed similar glass transition temperatures (T_g values). This might be explained by long alkyl spacer length between the main chain and mesogens. Since Young's modulus monotonically increases with an increase in the crosslinker content, the possibility of incomplete photopolymerzation can be excluded.

Despite the different phase behavior, the *cis*-azobenzene content of the samples in the photostationary state is in the same range: 59 , 61 , and 54 % for **P20**, **P60**, and **P100**, respectively (Figure 4). For all samples, the time evolution of the *cis*-azobenzene content can be fitted with a monoexponential function (solid lines in Figure 4) with time constants of ca. 7 s for **P20**, and ca. 15 s for **P60** and **P100**. At the same time, the birefringence of the samples is seen to decrease upon UV irradiation. The time dynamics of the decrease in birefringence correlates well with the increase in *cis*-azobenzene content for all the samples: once the photostationary value of the *cis*-azobenzene content is reached, the birefringence is also seen to reach its plateau value. The absolute change in birefringence is on the order of just a few percent, suggesting that the nonphotoactive mesogens remain largely unaffected by the photoisomerization process. This can be

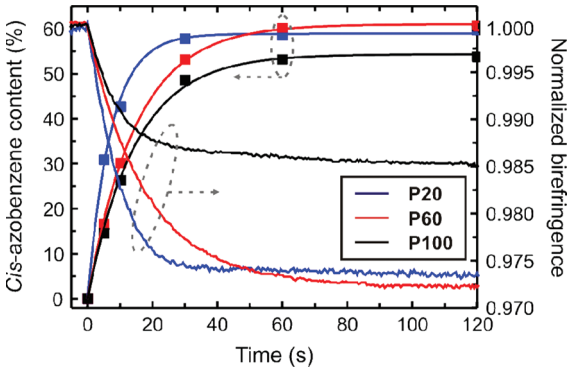

Figure 4. Time evolution of *cis*-azobenzene content and photoinduced change in birefringence upon UV irradiation (365 nm, 10 mW/cm^2) for **P20**, **P60**, and **P100**. For the *cis*-azobenzene content, the squares represent the measured values, and the solid line is a monoexponential fit to the experimental data.

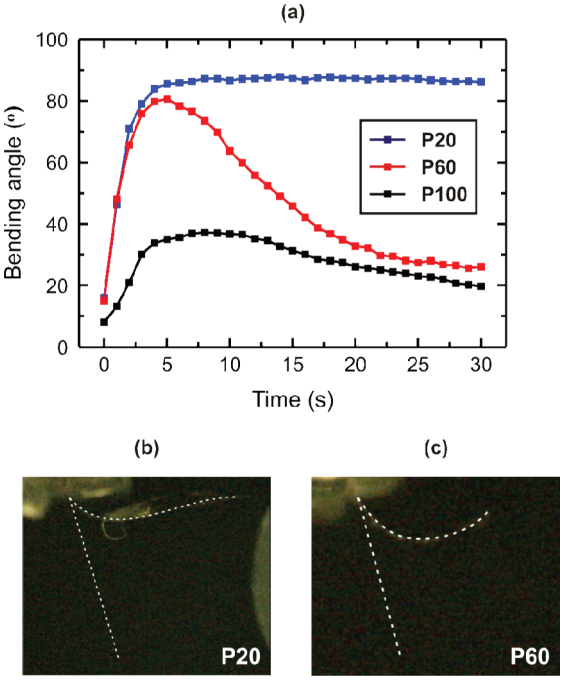

Figure 5. (a) Bending angle for **P20**, **P60**, and **P100** upon UV irradiation (365 nm, 10 mW/cm^2) as a function of time. (b) and (c); Photographs of **P20** and **P60** in the bent state. The dashed lines, drawn to guide the eye, show both the initial and the bent state of the films. The UV light is incident to the samples form the right. Because of the slight curling of the **P20**, its bending angle cannot be unambiguously determined. The value given in (a) represents the bending angle. Size of the films: 5 mm × 7 mm × 10 μm.

attributed to the low azobenzene concentration (5 mol %), due to which the isomerization process does not significantly distort the mesogen alignment even if the *cis*-azobenzene content in the photostationary state is on the order of 60 %.

Despite the small UV-light-induced change in birefringence, both **P20** and **P60** bent rapidly towards the light source even under low-intensity (10 mW/cm^2) UV irradiation, reaching the maximum bending angle within 5 s (Figure 5a), i.e., in a significantly shorter time than the time required for reaching the

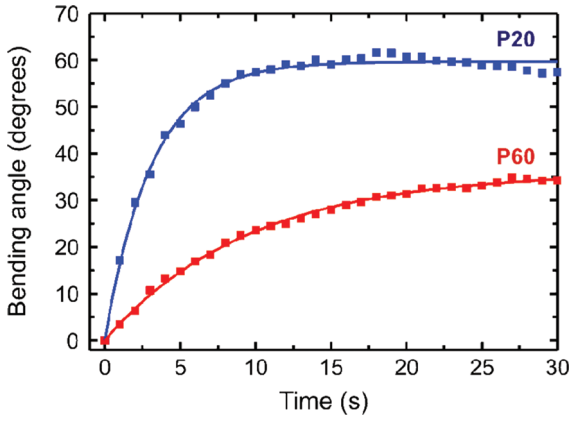

Figure 6. Bending angle of **P20** and **P60** as a function of time upon UV irradiation (365 nm, 10 mW/cm^2). The size of the films was 5 mm × 5 mm × 20 μm. The solid lines are monoexponential fits to the experimental data (squares).

maximum destruction in molecular alignment (Figure 4). **P100**, on the other hand, showed only weak bending compared to **P20** and **P60**. This suggests that the elastic properties play an important role in the photoinduced macroscopic motions of the cross-linked azobenzene-containing LC polymers: the lower the cross-linker concentration, i.e., the softer the material, the faster the bending process — as long as the azobenzene content is equal. Such behavior differs from samples composed of azobenzene mesogens only, where a high crosslinker concentration enhances the photoinduced stress and as well as the bending extent.[23−25] The behavior reported here only holds down to a certain lower limit of nonphotoactive cross-links: if the material system consists only of **DA9AB** (5 mol %) and **A9BZ9** (95 mol %), the bending is far less efficient than for **P20**.[35]

The bending behavior of **P20** and **P60** differed remarkably upon prolonged irradiation: whereas **P20** remained in the bent state during the 30 s monitoring period, **P60** (as well as **P100**) unbent after reaching the maximum bending angle upon 5 s UV exposure. We attribute the different behavior of **P20** and **P60** as follows. Because of its lower modulus, **P20** is more flexible to deform than the higher-modulus **P60**. Therefore, even if both samples bent almost by 90° toward the light source, their shape in the bent state is completely different (see Figure 5b): the highly flexible **P20** became almost parallel to the propagation direction of the incident light, and consequently it was almost unexposed to the UV light in the bent state.[36] **P60**, on the other hand, remained curved in the bent state (Figure 5c), allowing the gradient in the *cis*-azobenzene content to disappear upon prolonged exposure.[28,36] Such unbending behavior upon prolonged irradiation has been previously observed for cross-linked LC polymers with a low azobenzene concentration.[27,28] Here we note that for **P60**, the unbending occurs in the same time scale as it takes to reach the photostationary state in the *cis*-azobenzene content. Hence the results presented in Figures 4 and 5 point out important interrelations on the cause of the photoinduced unbending, showing explicitly that once the photostationary state in the *cis*-azobenzene content is reached, the gradient required to drive the asymmetric deformation of the film diminishes and the film becomes unbent. The maximum bending, on the other hand, is reached at significantly shorter time scales, reinforcing the fact that the maximum strain gradient drives the asymmetric photoinduced deformation and bending of the cross-linked azobenzene-containing LC polymers.

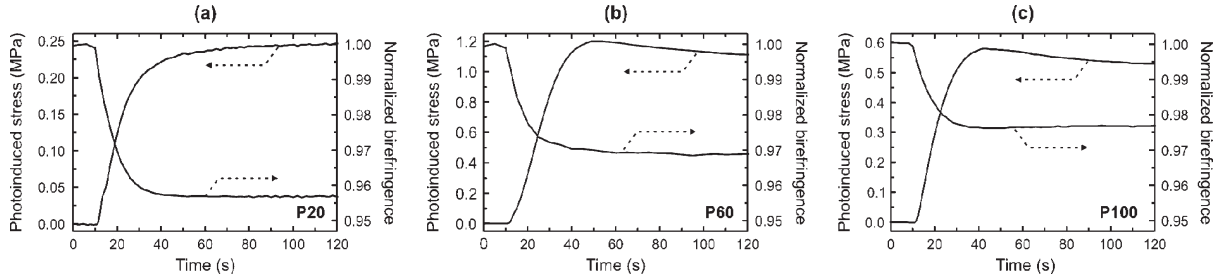

Figure 7. Photoinduced stress and change in birefringence for (a) **P20**, (b) **P60**, and (c) **P100** upon UV irradiation (365 nm, 10 mW/cm^2). The irradiation is started at 10 s.

Next, we studied the photomechanical properties of the polymers. These experiments were performed using 20 μm samples, as the 10 μm samples were too fragile to be clamped to the thermomechanical analyzer. Again, the bending of **P100** was small, whereas **P20** and **P60** bent towards the light source. As evident from Figure 6, the photoinduced bending process is slower for the 20 μm samples than for the 10 μm samples under similar irradiation conditions, and can be satisfactorily fitted with a monoexponential function during the monitoring period for both **P20** and **P60**. The time constants for the fitting are ca. 3 s for **P20** and ca. 10 s for **P60** (we note that also the bending dynamics of the 10 μm **P20** sample can be fitted with a monoexponential function, and the determined time constant is ca. 1.5 s). The bending was faster for **P20**, the sample with lower crosslinker concentration, than for **P60**. Note that for the 20 μm films, no unbending occurred during the monitoring period, which is consistent with our earlier work.[27] This can be attributed to the high absorbance of these films, which prevents the UV light to propagate through the sample. Hence, a strain gradient remains in the sample even in the photostationary state, and no unbending takes place.

Figure 7 presents the simultaneous measurement of photoinduced change in birefringence and photoinduced stress. Like the comparison between the *cis*-azobenzene content and photoinduced change in birefringence shown in Figure 4, the generated stress and the birefringence change followed the same time dynamics, whereas the bending angle reached the maximum at notably shorter time scale (for **P20**, the time constants for the monoexponential fitting are ca. 3 s for the photoinduced bending, and ca. 12 s for the photogenerated stress). This indicates that the molecular alignment in the film becomes (slightly) disordered by the trans−cis photoisomerization of the azobenzene moieties, and even the small distortion generates a notable stress into the cross-linked azobenzene-containing LC polymers. Note also that although the birefringence decrease is the largest for **P20**, its photogenerated stress is by far the lowest, only ca. 0.25 MPa, whereas the stress generated in **P60** and **P100** is ca. 1.2 and 0.6 MPa, respectively.

Compared to the photoinduced bending, photoinduced stress exhibited very distinct dependence on the crosslinker concentration. Although the bending angle was much larger for **P20** than for **P60**, the photogenerated stress was almost 5 times higher in the latter, being 1.2 and 0.25 MPa for **P60** and **P20**, respectively. Even the **P100** film exhibiting no significant bending produced 2.4 times higher stress than the **P20**. This suggests that a certain degree of elasticity promotes the photoinduced bending, whereas stiffer materials, preferably with moderate azobenzene concentration,[27] are favorable for generating high photoinduced stress.

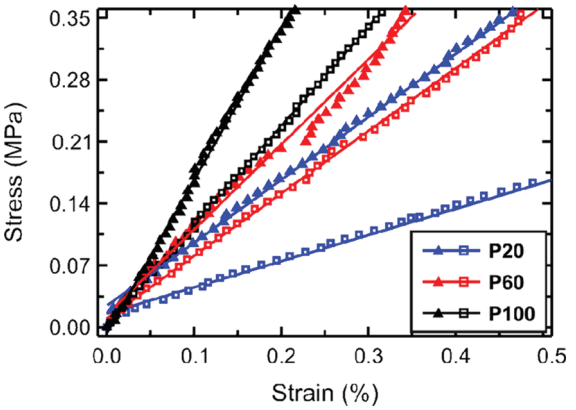

Figure 8. Stress−strain curves for nonexposed (filled triangles) and UV-irradiated (empty squares; 5 min irradiation, 365 nm, 10 mW/cm^2) films of **P20**, **P60**, and **P100**. The solid lines are linear fits to the experimental data, the slope of which are used to determine the Young's moduli of the samples. For clarity, only every fifth data point is shown.

The distinct nature of these two processes is further highlighted by their time dynamics for unlike photoinduced bending, the photogenerated stress closely follows the time evolution of the photoinduced change in the molecular alignment (Figure 7) and is thus inherently connected to the accumulation of the *cis*-azobenzenes throughout the bulk of the material system. Photoisomerization of the azobenzenes and the resultant photoinduced alignment change are necessary to cause bending and stress generation, but the maximum stress seems to be mainly controlled by the balance between elasticity and birefringence change.

To investigate the role of elastic modulus of the films on the photogenerated stress, stress-strain curves were measured before and during UV irradiation. As seen from the stress-strain curves shown in Figure 8, the modulus increased with increasing crosslinker concentration, as expected based on previous reports.[22,25] More importantly, we observed a remarkable decrease in the Young's modulus in the UV-irradiated films. The effect is more pronounced in the low-modulus **P20** as in samples with higher crosslinker concentration: the ratio E_{irrad}/E_{dark} is 0.41, 0.74, and 0.66 for **P20**, **P60**, and **P100**, respectively (E_{dark} and E_{irrad} are the moduli before and during UV irradiation, respectively). This observation points out, for the first time to the best of our knowledge, that the generation of *cis*-azobenzenes softens the whole film by UV irradiation, even when using only 5 mol % azobenzene concentration. It is interesting that the effect is the most prominent in **P20**, in which the modulus upon UV exposure is only 40 % of its initial value. We note that in the UV-irradiated

films, the measurement was performed after the photoinduced contration reached the photostationary state, indicating that the change in the slope truly reflects the photosoftening of the film.

Further time-dependent studies are required before making conclusive statements about the photosoftening, observed even in low-azobenzene-concentration cross-linked LC polymers. The simplest explanation would be that the *cis*-azobenzenes generated upon UV irradiation act as plasticizers, lowering T_g and hence the elastic modulus of the polymer. However, as the azobenzene concentration is only 5 mol %, we find it unlikely that the plasticization would account for such a large effect shown in Figure 8. Instead, we would like to highlight the recent work by Komp and Finkelmann who have shown using thermoelastic and X-ray investigations that defects may have a significant impact on the response of smectic-A LC networks to external strain, even if the LC phase structure remains unchanged upon the mechanical deformation.[37] We propose that in our highly ordered polymer network (for **P20**, $S \approx 0.75$), the generated *cis*-azobenzenes, which may induce local order−disorder transitons at their close proximity,[38] can be considered as such defects, which do not significantly distort the molecular alignment but alter the elastic properties of the material system in a highly nonlinear manner. The fact that the photoinduced change in Young's modulus is more pronounced in **P20** than in **P60**/**P100** could be explained by its higher initial ordering, rendering it more sensitive to photoinduced defect generation. We note, however, that further studies on the azobenzene concentration dependence and on the directional depencence of the photosoftening are necessary to verify this hypothesis.

We would also like to note that the photoisomerization-initiated softening has been widely studied in high-T_g amorphous polymers, to account for the possible connection between photosoftening and the formation of photoinduced surface-relief structures upon irradiation with coherent laser beams.[39−41] The results are somewhat controversial: the elastic modulus of amorphous azobenzene-containing polymers has indeed been reported to decrease upon light irradiation,[42] but the majority of the reports state that azo-polymer in fact hardens upon UV irradiation (which generates *cis*-azobenzenes into the polymer) while slight softening can be observed upon irradiation with visible light (which initiates *trans*−*cis*−*trans* cycling of the azobenzene chromophores).[43−46] On the other hand, recent studies by Yager and Barrett as well as by Mechau and Neher suggest that there is no significant change in the elastic modulus and viscosity upon laser illumination in high-T_g amorphous azo-polymers.[47,48] The pronounced difference between the results reported here (Figure 8) and those carried out using amorphous systems suggest that the photoinduced change in elasticity is inherently connected to the LC property of the polymer networks.

4. CONCLUSIONS

We have investigated the interrelation between photoisomerization, photoinduced change in molecular alignment, photoinduced stress, and macroscopic bending in cross-linked azobenzene-containing liquid-crystalline polymers. By performing simultaneous measurements of photogenerated stress and photoinduced change in birefringence, and by comparing the results to the photoinduced bending dynamics, we have explicitly showed that these two processes follow distinct time scales. Moreover, by studying samples of different crosslinker concentration, we point out that low Young's modulus is favorable for macroscopic deformation, whereas high modulus promotes the generation of high photoinduced stress into the material system. We also observed a significant − up to 2.5-fold − decrease in Young's modulus of cross-linked azobenzene-containing LC polymers upon UV irradiation, which we propose to be related to generation of "defects" (cis-isomers) into the homogeneously aligned cross-linked LC polymers. We believe that simultaneous monitoring of the alignment order and the photomechanical response serves as a useful tool for gaining fundamental understanding of the complicated physical processes governing the photomechanical response of azobenzene-containing cross-linked liquid-crystalline polymers.

AUTHOR INFORMATION

Corresponding Author
*E-mail: ashishid@res.titech.ac.jp.

REFERENCES

(1) Zhao, Y.; Ikeda, T., Eds. *Smart Light-Responsive Materials: Azobenzene-Containing Polymers and Liquid Crystals*; John Wiley & Sons: New York, 2009.
(2) Sekkat, Z.; Knoll, W., Eds. *Photoreactive Organic Thin Films*; Academic Press: San Diego, CA, 2002.
(3) Yager, K. G.; Barrett, C. J. *J. Photochem. Photobiol. A* **2006**, *182*, 250–261.
(4) Natansohn, A.; Rochon, P. *Chem. Rev.* **2002**, *102*, 4139–4175.
(5) Ikeda, T.; Mamiya, J.; Yu, Y. *Angew. Chem. Int. Ed.* **2007**, *46*, 506–528.
(6) Viswanathan, N. K.; Kim., D. Y.; Bian, S.; Williams, J.; Liu, W.; Li, L.; Samuelson, L.; Kumar, J.; Tripathy, S. K. *J. Mater. Chem.* **1999**, *9*, 1941–1955.
(7) Finkelmann, H.; Nishikawa, E.; Pereira, G. G.; Warner, M. *Phys. Rev. Lett.* **2001**, *87*, 015501.
(8) Hogan, P. M.; Tajbakhsh, A. R.; Terentjev, E. M. *Phys. Rev. E* **2002**, *65*, 041720.
(9) Li, M. H.; Keller, P.; Li, B.; Wang, X.; Brunet, M. *Adv. Mater.* **2003**, *15*, 569–572.
(10) Yu, Y.; Nakano, M.; Ikeda, T. *Nature* **2003**, *425*, 145.
(11) Harris, K. D.; Cuypers, R.; Scheibe, P.; van Oosten, C. L.; Bastiaansen, C. W. M.; Lub, J.; Broer, D. J. *J. Mater. Chem.* **2005**, *15*, 5043–5048.
(12) van Oosten, C. L.; Bastiaansen, C. W. M.; Broer, D. J. *Nat. Mater.* **2009**, *8*, 677–682.
(13) Cheng, F.; Yin, R.; Zhang, Y.; Yen, C.; Yu, Y. *Soft Matter* **2010**, *6*, 3447–3449.
(14) Yoshino, T.; Kondo, M.; Mamiya, J.; Kinoshita, M.; Yu, Y.; Ikeda, T. *Adv. Mater.* **2010**, *22*, 1361–1363.
(15) White, T. J.; Tabiryan, N. V.; Serak, S. V.; Hrozhyk, U. A.; Tondiglia, V. P.; Koerner, H.; Vaia, R. A.; Bunning, T. J. *Soft Matter* **2008**, *4*, 1796–1798.
(16) Serak, S.; Tabiryan, N.; Vergara, R.; White, T. J.; Vaia, R. A.; Bunning, T. J. *Soft Matter* **2010**, *6*, 779–783.
(17) Camacho-Lopez, M.; Finkelmann, H.; Palffy-Muhoray, P.; Shelley, M. *Nat. Mater.* **2004**, *3*, 307–310.
(18) Yamada, M.; Kondo, M.; Mamiya, J.; Yu, Y.; Kinoshita, M.; Barrett, C. J.; Ikeda, T. *Angew. Chem., Int. Ed.* **2008**, *47*, 4986–4988.
(19) Yamada, M.; Kondo, M.; Miyasato, R.; Naka, Y.; Mamiya, J.; Kinoshita, M.; Shishido, A.; Yu, Y.; Barrett, C. J.; Ikeda, T. *J. Mater. Chem.* **2009**, *19*, 60–62.
(20) Kondo, M.; Yu, Y.; Ikeda, T. *Angew. Chem., Int. Ed.* **2006**, *45*, 1378–1382.
(21) Yu, Y.; Maeda, T.; Mamiya, J.; Ikeda, T. *Angew. Chem., Int. Ed.* **2007**, *46*, 881–883.
(22) Lee, K. M.; Koerner, H.; Vaia, R. A.; Bunning, T. J.; White, T. J. *Macromolecules* **2010**, *43*, 8185–8190.

(23) Yu, Y.; Nakano, M.; Shishido, A.; Shiono, T.; Ikeda, T. *Chem. Mater.* **2004**, *16*, 1637–1643.
(24) Kondo, M.; Miyasato, R.; Naka, Y.; Mamiya, J.; Kinoshita, M.; Yu, Y.; Barrett, C. J.; Ikeda, T. *Liq. Cryst.* **2009**, *36*, 1289–1293.
(25) Zhang, Y.; Xu, J.; Cheng, F.; Yin, R.; Yen, C.; Yu, Y. *J. Mater. Chem.* **2010**, *20*, 7123–7130.
(26) Elias, A. L.; Harris, K. D.; Bastiaansen, C. W. M.; Broer, D. J.; Brett, M. J. *J. Mater. Chem.* **2006**, *16*, 2903–2912.
(27) Kondo, M.; Sugimoto, M.; Yamada, M.; Naka, Y.; Mamiya, J.; Kinoshita, M.; Shishido, A.; Yu, Y.; Ikeda, T. *J. Mater. Chem.* **2010**, *20*, 117–122.
(28) van Oosten, C. L.; Corbett, D.; Davies, D.; Warner, M.; Bastiaansen, C. W. M.; Broer, D. J. *Macromolecules* **2008**, *41*, 8592–8596.
(29) Harvey, C. L. M.; Terentjev, E. M. *Eur. Phys. J. E* **2007**, *23*, 185–189.
(30) Corbett, D.; Warner, M. *Phys. Rev. E* **2008**, *78*, 061701.
(31) Dunn, M. L. *J. Appl. Phys.* **2007**, *102*, 013506.
(32) Donnio, B.; Wermter, H.; Finkelmann, H. *Macromolecules* **2000**, *33*, 7724–7729.
(33) Andruzzi, L.; Apollo, F. D.; Galli, G.; Gallot, B. *Macromolecules* **2001**, *34*, 7707–7714.
(34) Fischer, E. *J. Phys. Chem.* **1967**, *71*, 3704–3706.
(35) Shimamura, A.; Hiraoka, T.; Kondo, M.; Kubo, S.; Mamiya, J.; Shishido, A.; Ikeda, T. *Mol. Cryst. Liq. Cryst.* **2010**, *529*, 53–59.
(36) We note here that photoinduced unbending did take place also for **P20**, but only after irradiation of several minutes (cf. the unbending took place in 10-20 s for **P60** and **P100**). We do not know the cause for such anomalously slow unbending, but tentatively propose that it is initiated by thermal cis−trans isomerization. Because of the high flexibility of the **P20** film, even minor thermal back isomerization can give rise to shape changes of the bent film, and consequently promote its interaction with the incident light. This could be a plausible cause for the observed slow unbending, even if detailed understanding on the connection between the elasticity and the photoinduced unbending requires further investigations.
(37) Komp, A.; Finkelmann, H. *Macromol. Rapid Commun.* **2007**, *28*, 55–62.
(38) Shishido, A.; Tsutsumi, O.; Kanazawa, A.; Shiono, T.; Ikeda, T.; Tamai, N. *J. Am. Chem. Soc.* **1997**, *119*, 7791–7796.
(39) Kim, D. Y.; Li, L.; Jiang, X. L.; Shivshankar, V.; Kumar, J.; Tripathy, S. K. *Macromolecules* **1995**, *28*, 8835–8839.
(40) Barrett, C. J.; Rochon, P. L.; Nathanson, A. L. *J. Chem. Phys.* **1998**, *109*, 1505–1516.
(41) Hennenberg, O.; Geue, Th.; Saphiannikova, M.; Pietsch, U.; Chi, L. F.; Rochon, P.; Nathansohn, A. L. *Appl. Phys. Lett.* **2001**, *79*, 2357–2359.
(42) Kim, H. K.; Wang, X. S.; Fujita, Y.; Sudo, A.; Nishida, H.; Fujii, M.; Endo, T. *Macromol. Chem. Phys.* **2005**, *206*, 2106–2111.
(43) Srikhirin, T.; Laschitsch, A.; Neher, D.; Johannsmann, D. *Appl. Phys. Lett.* **2000**, *77*, 963–965.
(44) Mechau, N.; Saphiannikova, M.; Neher, D. *Macromolecules* **2005**, *38*, 3894–3902.
(45) Moniruzzaman, M.; Zioupos, P.; Fernando, G. F. *Scr. Mater.* **2006**, *54*, 257–261.
(46) Richter, A.; Nowicki, M.; Wolf, B. *Mol. Cryst. Liq. Cryst.* **2008**, *483*, 49–61.
(47) Yager, K. G.; Barrett, C. J. *Macromolecules* **2006**, *39*, 9320–9326.
(48) Mechau, N.; Saphiannikova, M.; Neher, D. *Appl. Phys. Lett.* **2006**, *89*, 251902.